Probabilistic characteristics of strip footing bearing capacity evaluated by random finite element method

J. Pieczyńska, W. Puła
Institute of Geotechnics and Hydrotechnics, Wroclaw University of Technology, Poland
D.V. Griffiths
Division of Engineering, Colorado School of Mines, Golden, Colorado, USA.
G. A. Fenton
Dalhousie University, Halifax, Nova Scotia, Canada

ABSTRACT: The Random Finite Element Method has been employed for calculating the random characteristics of bearing capacity of a strip foundation. The study has been carried out for two different soils; a grey-blue clay from Taranto in Italy, which is well defined from a stochastic point of view, and a cohesionless soil with assumed stochastic characteristics. The authors have focused on developing a formulation, which includes anisotropic random fields of cohesion as well as the angle of internal friction. The effect of self weight has been incorporated for the first time in studying the bearing capacity of spatially variable soil. Results clearly show that the introduction of anisotropy into random fields is more realistic, and makes RFEM predictions more effective for design purposes.

1 INTRODUCTION

The design of shallow footings is often based on the evaluation of bearing capacity. The random character of the physical and mechanical soil properties heavily influences the randomness of the bearing capacity estimation, which is not usually taken into account into practice. However, some new building codes, such as Eurocodes, have suggested reliability-based design as a one of the possible design approaches. In this paper 2D numerical simulations are employed for the estimation of shallow footing bearing capacity in conjunction with the random finite element method (RFEM). The numerical methodology of RFEM was first introduced by Griffiths and Fenton (1993) for a seepage problem, and has since been employed in many applications (e.g. Griffiths and Fenton 2001, Fenton and Griffiths 2003, Griffiths et al. 2006, Fenton and Griffiths 2008). RFEM connects random field theory (Vanmarcke 1984) and deterministic finite element methods by taking into account the mean value, standard deviation, and correlation length of strength and other geotechnical parameters.

Usually bearing capacity design of shallow foundation utilizes the formula proposed by Terzaghi (1943).

$$q_f = cN_c + qN_q + \frac{1}{2}\gamma BN_\gamma, \tag{1}$$

where q_f is the ultimate bearing stress, c is the cohesion, q is the overburden load due to foundation embedment, γ is the soil unit weight, B is the footing width, and N_c, N_q and N_γ are the bearing capacity factors.

In earlier work, numerical algorithms created for RFEM by Fenton and Griffiths (2003) simplified the analysis and focused on the random character of soil parameters. The ultimate bearing stress (neglecting the contributions of both the footing embedment and the soil weight) was given by:

$$q_f = cN_c \tag{2}$$

where the N_c expression is given below (e.g. Bowles 1996):

$$N_c = \frac{e^{\pi \tan\phi} \tan^2\left(\frac{\pi}{4} + \frac{\phi}{2}\right) - 1}{\tan\phi} \tag{3}$$

Fenton and Griffiths (2003) have analyzed isotropic subsoil assuming that the spatial correlation is the same in both the vertical and horizontal directions. They have pointed out the presence of the so called “worst case”, which means that in every single situation it is possible to assign the characteristic value of correlation length corresponding to the most conservative evaluation of the bearing capacity.

In the paper by Cherubini *et al* (2009) an anisotropic random fields of soil properties has been incorporated. They considered an anisotropic random field of soil properties by implementing different values of correlation length in the vertical and horizontal directions.

In the present study the authors demonstrate for the first time, the effects of incorporating the self-weight of the soil under the foundation base in an RFEM analysis.

This corresponds to the extension of bearing stress formula to the form:

$$q_f = cN_c + \frac{1}{2}\gamma BN_\gamma \tag{4}$$

for cohesive soil and:

$$q_f = \frac{1}{2}\gamma BN_\gamma \tag{5}$$

for cohesionless soil.
Furthermore, the influence of the anisotropic character of random fields has been examined. Finally some analyses concerning the probability distributions of bearing capacity are presented.

2 THE RANDOM FIELD MODEL FOR SOIL PROPERTIES

The random soil model proposed by Fenton and Griffiths (2003) describes soil strength parameters by means of an isotropic two-dimensional random field by the local averaging approach (Fenton and Vanmarcke, 1990).

In the present paper two random fields are taken into account, one for c (cohesion) and one for ϕ (friction angle). The cohesion random field is assumed to be lognormally distributed with mean μ_c, standard deviation σ_c and different spatial correlation lengths θ_{cy} and θ_{cx} in vertical and horizontal direction, respectively.

Theoretical aspects of the anisotropic random field assumption have been analyzed in earlier papers (Puła and Shahrour 2003, Puła 2004).

The lognormal random field is derived from a normally distributed random field $G_{\ln c}(\mathbf{x})$, having zero mean, unit variance and spatial correlation length $\theta_{\ln c}$ transformed as follows:

$$c(\mathbf{x}) = \exp\left\{\mu_{\ln c} + \sigma_{\ln c} G_{\ln c}(\mathbf{x})\right\} \tag{6}$$

where $\mathbf{x}$ = the spatial position at which c is calculated and $\mu_{\ln c}$ and $\sigma_{\ln c}$ are mean and standard deviation values of (log) cohesion function:

$$\sigma^2_{\ln c} = \ln\left(1 + \frac{\sigma_c^2}{\mu_c^2}\right) \tag{7}$$

$$\mu_{\ln c} = \ln \mu_c - \frac{1}{2}\sigma^2_{\ln c}\,. \tag{8}$$

Such a transformation is very useful because there are many effective methods for generating normal field and then using Monte Carlo simulation. Realizations of cohesion field have been calculated after having generated the realization of normal field using the transformation in Eq. (6). Correlation structure of cohesion lognormal field $G_{\ln c}(\mathbf{x})$ is expressed by determining the correlation function, whose parameters are correlation lengths along the two directions $\theta_{(\ln c)y}$ and $\theta_{(\ln c)x}$.
In this paper the following correlation function has been assumed:

$$\rho_{\ln c} = \exp\left(-\sqrt{\left(\frac{2(\tau_2)}{\theta_{(\ln c)x}}\right)^2 + \left(\frac{2(\tau_1)}{\theta_{(\ln c)y}}\right)^2}\right) \tag{9}$$

where $\tau_1 = y_2 - y_1$ and $\tau_2 = x_2 - x_1$ are the two components of the absolute distance between the two points in 2D space where the correlation function is calculated by taking into account the anisotropic character of the random field ($\theta_{(lnc)x}$ and $\theta_{(lnc)y}$). It is worth mentioning that such a correlation function works in a normal random field *ln c*. $\theta_{(\ln c)y}$ and $\theta_{(\ln c)x}$ values are derived from θ_{cy} and θ_{cx} values. Correlation lengths θ_{cy} and θ_{cx} can be drawn from in situ tests. One method for converting soil testing results into correlation length is the moment method (Baecher and Christian 2003). Such methodology has been used in this paper. The different between isotropy and anisotropy random field are illustrated in Figure 1.

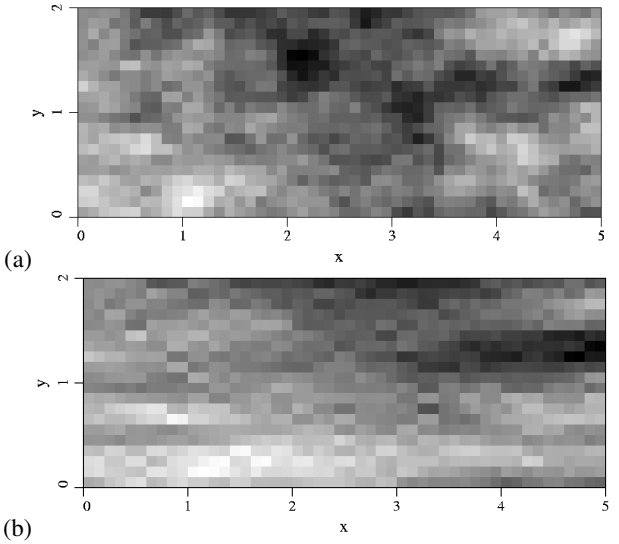

Figure 1. Analyzed mesh of (a) isotropic soil with θ_x=*0.5*, θ_y=*0.5;* (b) anisotropic case with θ_x=*5.0*, θ_y=*0.5.* The darker regions indicate weaker soil.

The larger value of horizontal correlation length seems to imitate more realistic natural soil property (Figure 1). In-situ tests have demonstrated that the horizontal correlation length is significantly greater than the vertical one (Cherubini 1997).

The second random field considered in this paper is the friction angle. Since friction angle values change within a bounded interval, neither normal nor lognormal distributions are appropriate models for random variable. Fenton and Griffiths (2003) represented bounded of "tanh" distributed fields as a bounded distribution, which arises as a simple transformation of a $G_\phi(\mathbf{x})$, according to:

$$\phi(x) = \phi_{\min} + \frac{1}{2}\left(\phi_{\max} - \phi_{\min}\right)\left\{1 + \tanh\left(\frac{sG_{\phi}(x)}{2\pi}\right)\right\} \qquad (10)$$

where ϕ_{min} and ϕ_{max} are the minimum and maximum values of friction angle, respectively, and s is the scale factor depending on standard deviation.

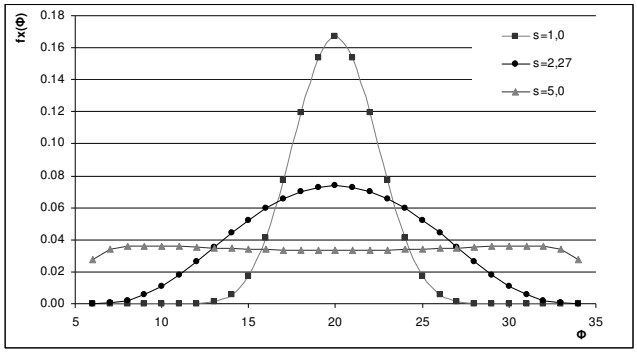

Figure 2. Shapes of friction angle distribution of bounded type. The curve corresponding to $s=2,27$ ($\phi_{min}=5^{\circ}$; $\phi_{max}=35^{\circ}$; σ_{ϕ} = 4.8°) is the density of the distribution used in this paper for computations (grey-blue clay from Taranto).

Shapes shown in Figure 2 represent probability distribution functions of ϕ variable. In the graph, ϕ functions are reported for three different scale factor values s. For s values greater than 5 frequency distribution leads to a U-shaped function which is unrealistic in current situations. The mean distribution is in the middle of the interval [ϕ_{min}; ϕ_{max}]. Relationship between the standard deviation and the scale parameter s has no analytic form. It can be obtained by numerical integration or by Taylor's expansion. The first order approximation leads to:

$$\sigma_{\phi} \approx \frac{1}{2}\left(\phi_{max} - \phi_{\min}\right)\frac{2s}{\pi\left(\exp(2\phi_0) + \exp(-2\phi_0) + 2\right)} \qquad (11)$$

where ϕ_0 is the mean value of the friction angle. Correlation function and correlation length values have been estimated as in the case of cohesion.

As first soil the blue-grey clay has been considered. This kind of clay appears near the Taranto in South East of Italy. It has been widely described and statistically tested by Cherubini *et al* (2007) and applied to RFEM computations reported in the paper by Cherubini *et al* (2009). The random field characteristics have been synthesized in Table 2 as a result of investigation over Taranto blue-grey clay (Cherubini et al. 2007, 2009).

Table 2. Random characteristics of grey-blue clay.

Variable	Probability distribution	Mean	Standard deviation	Scale of fluctuation
		μ	σ	θ_y
c	Lognormal	36kPa	20kPa	0.2; 0.5; 0.7; 1.0 m
ϕ	Bounded (see Eq. (10))	20°	4.8°	0.2; 0.5; 0.7; 1.0 m
γ	Non-random	19 kN/m^3	-	-

*Horizontal fluctuation scale will be a subject of the parameter study.

The friction angle has been defined as being symmetric bounded distributed with lower limit $\phi_{min}=5^{\circ}$, upper limit $\phi_{max}=35^{\circ}$ and scale parameter $s=2.27$.

In the case of cohesionless soil a sand has been considered with bounded distribution of friction angle. The parameters of probability distribution are given in Table 3. The minimal and maximal values were equals to $\phi_{min}=14^{\circ}$, $\phi_{max}=51^{\circ}$ respectively and the scale parameter equal to $s=2.21$. The sand characteristics are synthetic input data and they are not reflect any specified real situation. They have been accepted on some literature analyses. In order to compare results the values of vertical fluctuation scale has been assumed the same as in the case of Taranto clay.

Table 3. Random characteristics of sand.

Variable	Probability distribution	Mean	Standard deviation	Scale of fluctuation*
		μ	σ	θ_y
ϕ	Bounded (see Eq. (10))	32.5°	4.8°	0.2; 0.5; 0.7;1.0 m
γ	Non-random	19 kN/m^3	-	-

*Horizontal fluctuation scale will be a subject of the parameter study.

3 RANDOM FINITE ELEMENT METHOD

The bearing capacity analysis carried out in this paper uses an elastic perfectly plastic stress strain law with a classical Mohr Coulomb failure criterion according to Fenton and Griffiths (2003) work. Plastic stress redistribution is accomplished using a viscoplastic algorithm. The program uses 8 node quadrilateral elements and reduced integration in both the stiffness and stress redistribution parts of the algorithm. The theoretical basis of the method is described in detail in Chapter 6 of the book by Smith and Griffiths (2004). The finite element model incorporates five parameters: Young's modulus (E), Poisson's ratio (ν), dilation angle (ψ), shear strength (c), and friction angle (ϕ). In the present study E, ν and ψ are held constant (at 60 MPa for grey-blue clay and 100 MPa for sand, $\nu = 0.3$, and $\psi = 0$ in both cases) while c and ϕ are randomized. Setting the dilation angle to zero means there is no plastic dilation during yield of the soil. This is the case in the following computations. The Young's modulus governs the initial elastic response of the soil, but does not affect the bearing capacity. Thus such elastic soil parameter has been used for pre-analyzing the system.

In order to check the correctness of the mesh model an analysis of the mesh influence on the bearing capacity mean value has been carried out. Figure 3 presents the bearing capacity average computed for finite element mesh consists of 20 and 30 elements in y-direction direction versus variable numbers of element in x-direction. It can
be observed that for a number of elements greater than 50 (in x-direction) the average of the bearing capacity becomes stable and at 50 reaches its minimal value.

Similar effects have been observed in the case in which the number of elements in y-direction is changing. The effects are illustrated in Figure 4. All computations in this case have been carried out with 50 elements in x-direction. The stabilization begins at 15, but the minimal value is observed at 20.

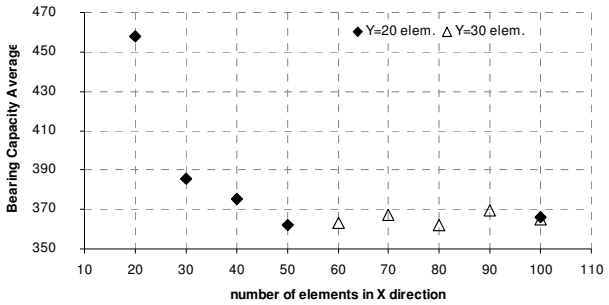

Figure 3. Bearing capacity average versus number of element in x-direction.

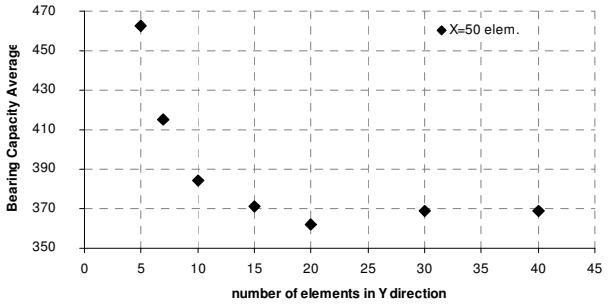

Figure 4. Bearing capacity average versus number of element in y-direction.

According to results presented in Figure 3 and Figure 4, the mesh of size 50 x 20, is accepted for further investigations (Figure 5). Each element is a square of side length 0.1 m and the strip footing occupies 10 elements, thus giving a width of B = 1 m.

The random fields in this study are generated using the Local Average Subdivision (LAS) method (Fenton and Vanmarcke 1990, Fenton and Griffiths 2008). Numerical analyses of the bearing capacity have been carried out according to numerical simulations by first two moments (mean and variance). In order to check the speed of convergence in simulation process the computations were carried out for different number of realizations (samples). Results for sample size 300, 500 and 1000 are reported in Figure 6. There, the confidence intervals considered with selected exceeding probability $\alpha = 0.05$ are as follows: lower bound of mean value: 450.22 kPa, upper bound of mean value: 481,00 kPa; lower bound of standard deviation: 164,67 kPa, upper bound of standard deviation: 186,46 kPa. Accordingly the optimum number of realizations turned out to be 300; whereas more than 1000 realizations are needed to determine the approximate form of the bearing capacity distribution. As a next step an effect of cross-correlation of strength parameters has been investigated. Since a negative cross-correlation, has been experimentally established for many soil types the computations have been repeated for three negative correlation coefficients: ρ = - 0.7, ρ = - 0.5, ρ = - 0.3. Examples of results are presented in Figure 7 (mean values) and Figure 8 (standard deviations).

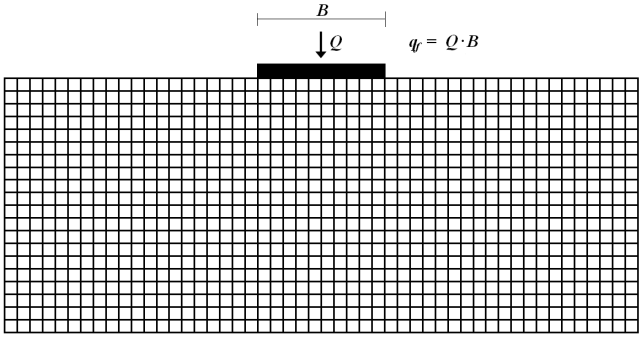

Figure 5. Mesh model used in stochastic bearing capacity predictions (After Griffiths and Fenton 2001)

Figure 6 Testing of convergence rate for mean value of bearing capacity. Runs have been started from three different seeds.

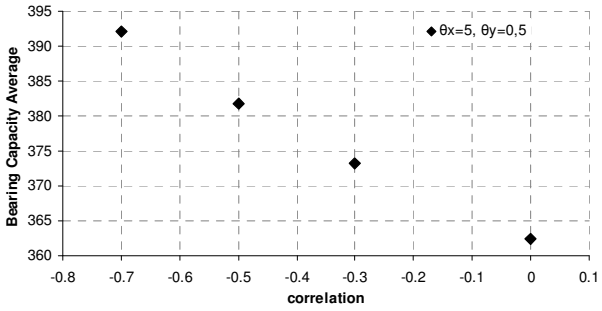

Figure 7. Average bearing capacity versus cross-correlation coefficient of strength parameters φ and c.

It is easy to see that for lack of correlation the average bearing capacity is the lowest and the standard deviation is the greatest. Therefore in the further computations the zero-value cross-correlation case has been selected. However, if the given negative value of the correlation coefficient is confirmed then including it in reliability computations would lead to more optimal evaluations. As it has been already mentioned computations within this study, has been carried out for anisotropic random fields. It means that the horizontal correlation length differs from the vertical one. In vertical direction, four values of correlation length θ_y have been considered: 0.2; 0.5; 0.7 and 1.0 m.

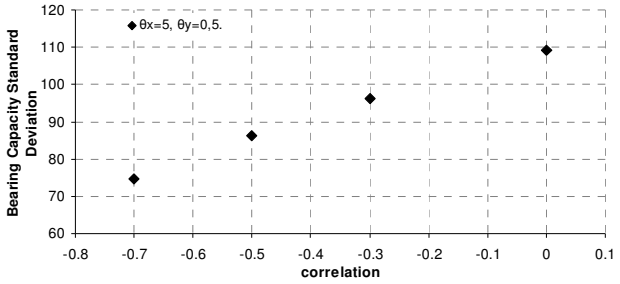

Figure 8. Bearing capacity standard deviation versus cross-correlation coefficient of strength parameters φ and c.

As it is reported in the literature (e.g. Cherubini 1997) the horizontal correlation length is much greater then vertical. Therefore the following values of θ_x were used in the computations: 1; 5; 10; 50 m. It was assumed that the correlation lengths of cohesion and friction angle are the same. Results for gray-blue clay are shown in Table 4. These results are also graphically presented in Figures 9 and 10. Additionally figures contain results for cases where the self-weight of the soil has been not included.

Table 4. Mean values and standard deviations of bearing capacity obtained in computations.

θx [m]	θy [m]	μqfi [kPa]	σqfi [kPa]	θx [m]	θy [m]	μqfi [kPa]	σqfi [kPa]
1	0.2	406.91	61.98	10	0.2	424.34	96.98
	0.5	399.79	83.79		0.5	423.94	133.46
	0.7	401.67	92.47		0.7	427.83	149.95
	1.0	406.67	102.48		1.0	435.13	171.05
5	0.2	416.22	89.61	50	0.2	434.80	102.23
	0.5	411.23	123.54		0.5	442.17	143.10
	0.7	413.48	138.03		0.7	450.05	160.65
	1.0	418.34	152.94		1.0	461.24	181.53

Figure 9 shows the obvious result that bearing capacity values increases if the self-weight of soil is incorporated. Standard deviation rises as the vertical correlation length increases. One can observe that the effect of horizontal fluctuation scale is important. However, for larger values that are realistic in natural soils, the bearing capacity coefficient of variations seems to be not very sensitive to the increase in the horizontal scale value (Figure 10). This result can be valuable if we are not able to precisely determine the horizontal fluctuation scale. Very important feature can be observed in Figure 10. Namely the coefficients of variation for cases with and without self-weight almost coincide, for the same values of fluctuation scale. On the other hand bearing capacity coefficient of variation stabilizes with respect to horizontal fluctuation scale, when this scale reaches high values.

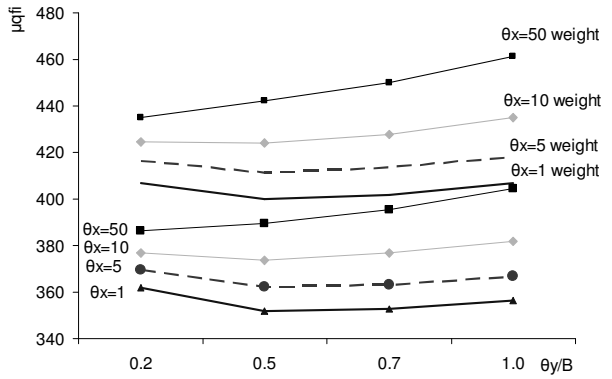

Figure 9. Mean value of bearing capacity versus ratio θy/B for different values of horizontal fluctuation scale. Curves denoted by θx weight result from computation where self-weight is included. Curves denoted by θx come from computation without including of self-weight.

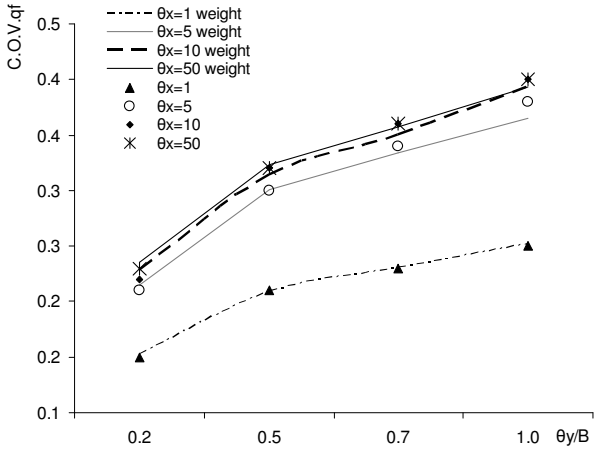

Figure 10. Coefficient of variation of bearing capacity versus ratio θy/B for different values of horizontal fluctuation scale. Curves denoted by θx weight result from computation where self-weight is included. Points denoted by θx come from computation without self-weight.

Let us now turn to the computations carried out for sand of characteristic presented in Table 3. In this case the self-weight of the subsoil has been incorporated in FEM computations. The results of computations are presented in the Table 5, Figure 11 and Figure 12. They show that changes in the mean value due to variation of the horizontal fluctuation scale are quite small. They appeared to be far smaller than in the cohesive soil. This result seems to be optimistic if we are not able to precisely determine the horizontal fluctuation scale.

Quite unexpected behavior can be observed when the coefficients of variations are analyzed. The Figure 12 shows that bearing capacity coefficients of variation may decrease with increasing value of horizontal fluctuation scale. This is in opposition to results for cohesive soil (see comparison given in Table 6) as well as results reported in earlier papers (Cherubini *et al* 2009, Pieczyńska & Puła 2009).

Table 5. Mean values and standard deviations obtained in cohesionless soil

θx [m]	θy [m]	μqfi [kPa]	σqfi [kPa]	θx [m]	θy [m]	μqfi [kPa]	σqfi [kPa]
1	0.2	67.23	18.55	10	0.2	68.95	20.17
	0.5	65.94	19.28		0.5	69.46	23.02
	0.7	65.78	19.53		0.7	70.30	24.45
	1.0	65.35	19.47		1.0	70.84	24.78
5	0.2	68.79	20.32	50	0.2	69.68	20.13
	0.5	68.83	22.74		0.5	69.33	21.24
	0.7	69.25	23.51		0.7	69.80	22.06
	1.0	70.21	24.75		1.0	70.70	22.85

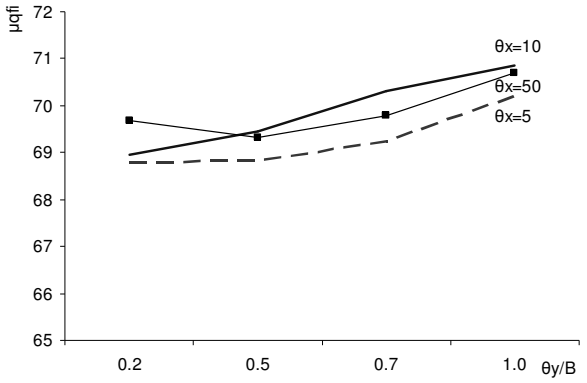

Figure 11. Mean value of bearing capacity versus ratio θy/B for different values of horizontal fluctuation scale. Results for cohesionless soil include self-weight.

It is recognized that finite elements computation of the bearing capacity of cohesionless soil is more challenging than cohesive soil, so this contrasting behavior needs further investigation and research.

4 PROBABILITY DISTRIBUTION OF BEARING CAPACITY

Probability based design are far easier to perform if a complete probability information of bearing capacity is known. This means that that it is worth to estimate the probability density function (or cumulative distribution function) of bearing capacity. In order to examine probability distributions for both – the blue-grey clay and sand Monte Carlo simulations have been carried out with the sample size of 2000.

For both cases (the blue-grey clay and the sand) vertical and horizontal fluctuation scales were equaled to θ_y = 0.7 m and θ_x = 50 m, respectively. The basic statistical parameters of samples are collected in Table 7 and Table 8 for the case of blue clay and the sand, respectively. Cumulative distribution functions have been matched by means both the method of moments and the least square method. It has appeared that estimation by lest squares had given better matching.

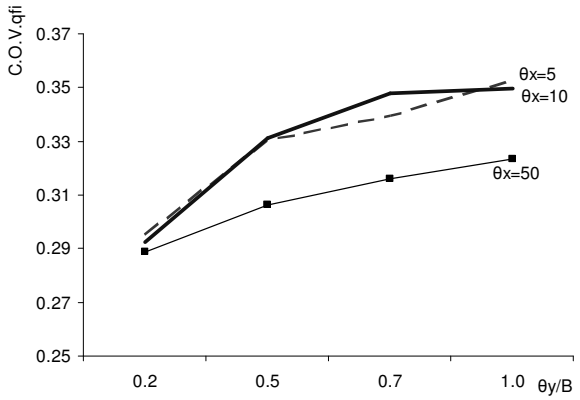

Figure 12. Coefficient of variation of bearing capacity versus ratio θy/B for different values of horizontal fluctuation scale. Results for cohesionless soil include self-weight.

Table 6 Comparison coefficients of variation for soil with and without cohesion.

θx [m]	θy [m]	C.O.V.qfi Cohesive	C.O.V.qfi Cohesionless
1	0.2	0.15	0.28
	0.5	0.21	0.29
	0.7	0.23	0.30
	1.0	0.25	0.30
5	0.2	0.22	0.30
	0.5	0.30	0.33
	0.7	0.33	0.34
	1.0	0.37	0.35
10	0.2	0.23	0.29
	0.5	0.31	0.33
	0.7	0.35	0.35
	1.0	0.39	0.35
50	0.2	0.24	0.29
	0.5	0.32	0.31
	0.7	0.36	0.32
	1.0	0.39	0.32

Table 7. Bearing capacity statistical parameters. The blue-grey clay case (the self-weight of the soil is included).

Minimum	93.20	Maximum	1180
Range	1086.8	Median	414.00
Arithmetic mean	441.64	Geometric mean	414.05
Mean square	25661.0	Variance	25673.0
Stand. deviation	160.23	Coef. of variation	0.36281
Third moment	3624300	Stand. Skewness	0.8817
Fourth moment	2.72E+09	Stand. kurtosis	4.1376
Variance of mean	12.83	Var. of variance	3.71E+15
Var. of 3. moment	2.10E+11	Var. of 4. moment	1.19E+17

Figure 13 shows result obtained for the blue-grey clay case in the form of histogram (simulation) and the estimated lognormal probability density function (the least square method).

Table 8. Bearing capacity main statistics for cohesionless soil included soil weight term.

Minimum	15.90	Maximum	192.00
Range	176.10	Median	70.40
Arithmetic mean	69.051	Geometric mean	64.789
Mean square	537.53	Variance	537.79
Stand. deviation	23.190	Coef. of variation	0.33584
Third moment	4343.0	Stand. skewness	0. 34849
Fourth moment	1.117E+06	Stand. kurtosis	3.8670
Variance of mean	0.26876	Var. of variance	0.623E+09
Var. of 3. moment	0.200E+07	Var. of 4. moment	0.303E+11

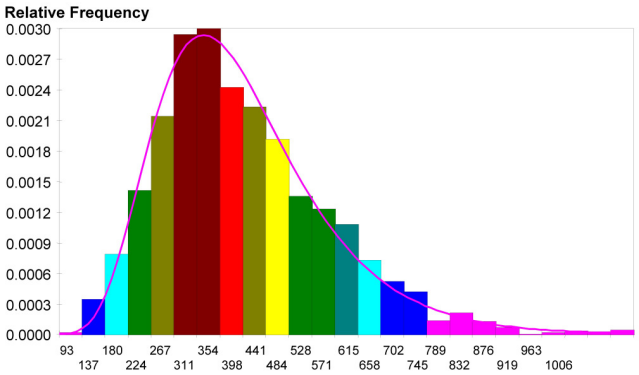

Figure 13. Density function with matching a lognormal distribution. Data set in Tables 7 and 9.

In Figure 14 the “empirical" cumulative distribution function received in the simulation is compared with the lognormal cumulative distribution function estimated by the least square method. It can be observed that both graphs almost coincide, which means a very good fitness. Next distribution hypotheses have been examined by statistical goodness-of-fit tests, namely the Kolmogorov-Smirnov test, chi-square test and Anderson-Darling test. The test results are demonstrated in the Table 9. All three goodness-of-fit tests show that there is no reason to reject the hypothesis that the bearing capacity for the case considered is lognormally distributed with the mean value equal to $E[q_f] = 440.46$ and the standard deviation $\sigma_q = 159.8$ (the least square fitness). It is worth mentioning that distributions fitted by the method of moments and fitted by the least squares method only slightly differ.

Another shape of the distribution has been obtained when the bearing capacity of the sand has been considered. The lognormal density appeared to be not well-fitted as shown in Figure 15. Several distributions have been tested for estimating simulated distribution, but none of them has given good result. Relatively well-fitness has been obtained by applying a normal distribution. Estimated by the least square normal p.d.f with the simulated histogram is presented in Figure 16 and the empirical and theoretical cumulative distributions functions are plotted in Figure 17.

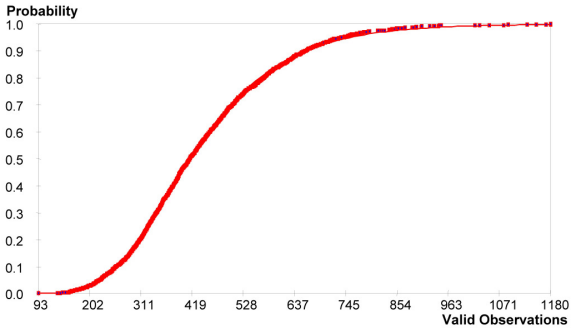

Figure 14. Lognormal cumulative distribution function compared with the empirical cumulative distribution function resulting from simulation.

Table 9. Tests for the estimation of the bearing capacity probability distribution for cohesive soil included soil weight term.

Parameter estimation for the case of 50m horizontal and 0.7m vertical scale of fluctuation			
Selected estimation method	Parameter 1 [xi]	Parameter 2 [delta]	Selected stochastic model
Method of moments	415.157	0.351652	Lognormal
Least square	414.050	0.364463	Lognormal
Testing			
Selected testing method		Kolmogorov-Smirnov test	
	Significance level	Critical significance level	
Method of moments	0.34012	0.05	
Least square	0.77108	0.05	
	The hypothesis should not be rejected.		
Selected testing method		Chi-square distribution test	
	Number of classes used in test	Significance level	Critical significance level
Method of moments	44	0.16868	0.05
Least square	44	0.18426	0.05
	The hypothesis should not be rejected.		
Selected testing method		Anderson-Darling test	
	Significance level	Critical significance level	
Method of moments	>0.15	0.05	
Least square	>0.15	0.05	
	The hypothesis should not be rejected.		

Figures 16 and 17 suggest that the normal fitness seems to be satisfactory for this case. As in the previous case statistical goodness-of –fit testing has been carried out. In the case, however, only Darling-Anderson test suggested to not reject the normality hypothesis.

Both the Kolmogorov-Smirnoff test ant the chi-square test suggested that the hypothesis should be rejected.

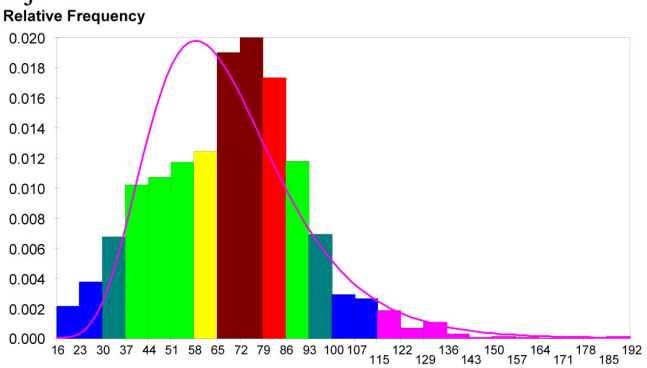

Figure 15. Density function with matching a lognormal distribution. Data set in Table 8.

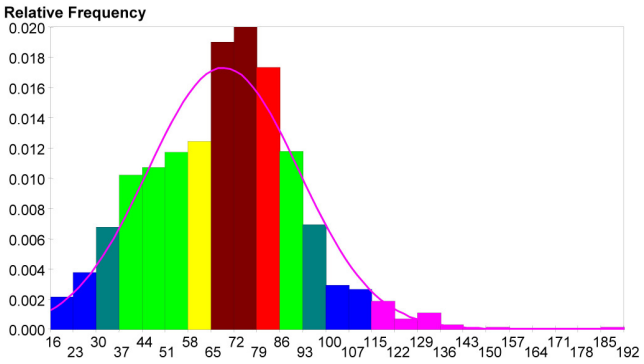

```
ERROR: stackunderflow
OFFENDING COMMAND: ~

STACK:
```